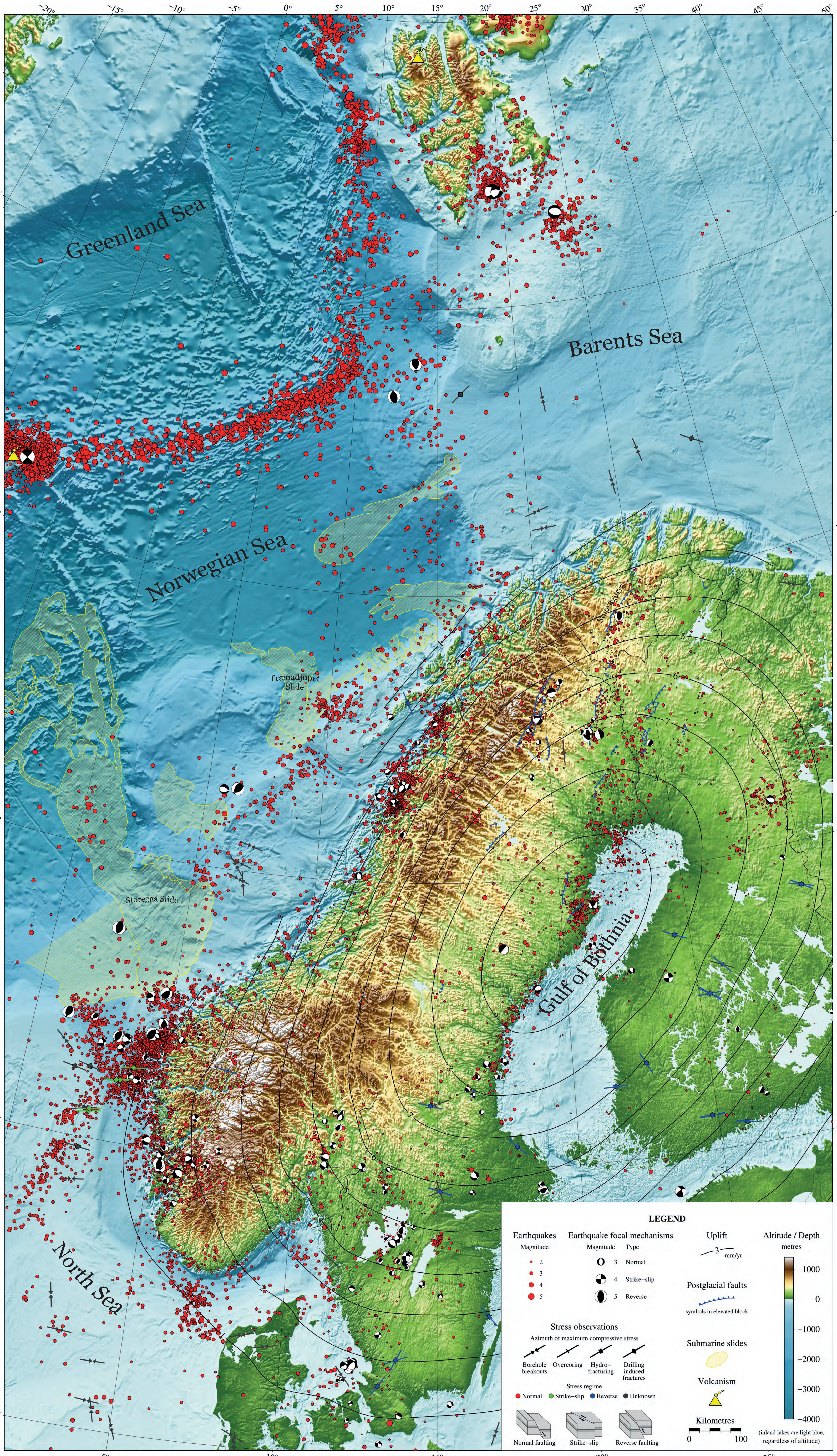

NEOTECTONIC MAP

NORWAY AND ADJACENT AREAS

Scale: 1:3 000 000

MAP DESCRIPTION

The mapped area includes Norway, Denmark, Sweden, Finland, Svalbard and part of the North Sea, the Norwegian Sea, the Greenland Sea and the western Barents Sea.

Neotectonics is the study of motion and deformation of Earth's crust that are current or recent in geologic time, here considered to be the Neogene and the Quaternary. Figure 1 shows Neogene deformation, while the main map and Figures 2 and 3 show Quaternary deformation.

There are nine major components of neotectonic deformation in the map area:
1. Oceanic spreading in the Norwegian-Greenland Sea
2. Neogene uplift and erosion of the mainland, Svalbard and the Barents Sea
3. Pliocene-Pleistocene deposition on the Norwegian margin
4. Submarine slides on the Norwegian margin
5. Quaternary volcanism on Svalbard and Jan Mayen
6. Quaternary glacial isostatic adjustment
7. The postglacial Lapland Fault Province
8. The state of stress
9. Seismicity

1. Oceanic spreading

Spreading in the Norwegian-Greenland Sea initiated in early Eocene (Talwani and Eldholm, 1977). The ridge push force from the oceanic spreading ridges probably causes NW-SE compressive stresses in Fennoscandia.

2. Neogene uplift and erosion

South Norway and Lofoten were uplifted approximately 1 km during the Neogene, mainly during Pliocene-Pleistocene (Fig. 1). The corresponding erosion of the coastal areas is estimated to have reached a maximum of 800-1000 m in South Norway and slightly more in Lofoten (Riis, 1996). The Barents Sea and Svalbard have been subject to considerable uplift and erosion, with a maximum of about 3 km on Svalbard (Henriksen et al., 2011).

3. Pliocene-Pleistocene deposition

Thick sediment packages were deposited on the Norwegian margin due to the uplift and erosion during the Pliocene-Pleistocene (Fig. 1). The thickest sediment packages of approximately 3 km were deposited in the northern Norwegian Sea (Faleide et al., 1996). Most of the deposition probably occurred due to glacial processes during the Quaternary.

4. Submarine slides

Large submarine slides are abundant along the Norwegian margin, and a number of these occurred during the Quaternary (Evans et al., 2005), as shown in the map. Two huge slides occured in recent time: the Trænadjupet slide dated to 4 000 yrs B.P (Laberg et al., 2000) and the Storegga slide at 8 200 yrs B.P. (Solheim et al., 2005).

5. Volcanism

In northern Spitsbergen, Svalbard, there are several Quaternary volcanic extrusives and dykes. The best known of these is the Sverrefjellet volcano, which erupted around 1 My B.P. (Treimann, 2012). The volcanic island Jan Mayen hosts an active volcano, the Beerenberg volcano, which had its last eruption in 1970.

6. Glacial isostatic adjustment

The Quaternary glaciations caused repeated loading and unloading of the lithosphere beneath Fennoscandia. Today, the region is still uplifting due to the glacial isostatic adjustment following the last deglaciation which ended around 11 500 yrs B.P. The map shows contours from a land uplift model based on GPS observations and levelling and a geophysical model of the glacial isostatic adjustment (Vestøl et al., 2016). The present-day uplift has a maximum of around 10 mm/yr in the Gulf of Bothnia and causes extensional horizontal strain rates in most of Fennoscandia (Fig. 2, Keiding et al., 2015).

7. The postglacial Lapland Fault Province

A number of pronounced postglacial fault scarps are present in northern Fennoscandia (e.g. Lagerbäck and Sundh, 2008; Olesen et al., 2013; Sutinen et al., 2014). Several of the scarps have confirmed reverse displacement, and many are located in older weakness zones. The reverse Stuoragurra fault in Norway can be followed for more than 80 km (Fig. 3).

The fault scarps probably formed due to an extraordinary pulse of seismicity, including a number of M>7 earthquakes, which occurred around the end of the last deglaciation. The seismicity is thought to have been triggered by the glacial unloading of the crust, which allowed the long-term compressive stress from plate tectonic forces to be released, perhaps aided by high pore pressures due to melt water percolating into the crust (Muir Wood, 1989). During recent years, Swedish and Finnish fault scarps and associated landslides have been mapped in detail using LiDAR (e.g. Mikko et al., 2015; Palmu et al., 2015).

8. The state of stress

Stress observations from measurements in deep boreholes are shown as azimuth of the maximum compressive stress from the World Stress Map database (Heidbach et al., 2016) as well as new data in Nordland (Olesen et al., 2018). A trend of NW-SE compressive stress is apparent on the Norwegian margin and in large parts of Fennoscandia, whereas other regions such as the Barents Sea and the North Sea show considerable variation in stress azimuth.

Indirect stress observations are obtained from earthquake focal mechanisms. The map shows a compilation of Norwegian, Swedish and Finnish earthquake focal mechanisms (Keiding et al., 2015) as well as new focal mehanisms in Nordland (Olesen et al., 2018). On the continental margin, the focal mechanisms typically indicate reverse faulting with NW-SE compressive axes. On land, the focal mechanisms indicate a larger variation between strike-slip, reverse and normal faulting.

9. Seismicity

The map shows earthquake locations and magnitudes during 1980–2012 (FENCAT, 2018). The present-day seismicity in Fennoscandia is low to intermediate, with the highest moment release along the continental margin and in western Norway. Earthquakes occur at relatively large depths of 10-30 km on the continental margin and at shallower depth on land. The largest historical earthquake in mainland Norway was the 31 August 1819 Lurøy earthquake in Nordland with MS=5.8.

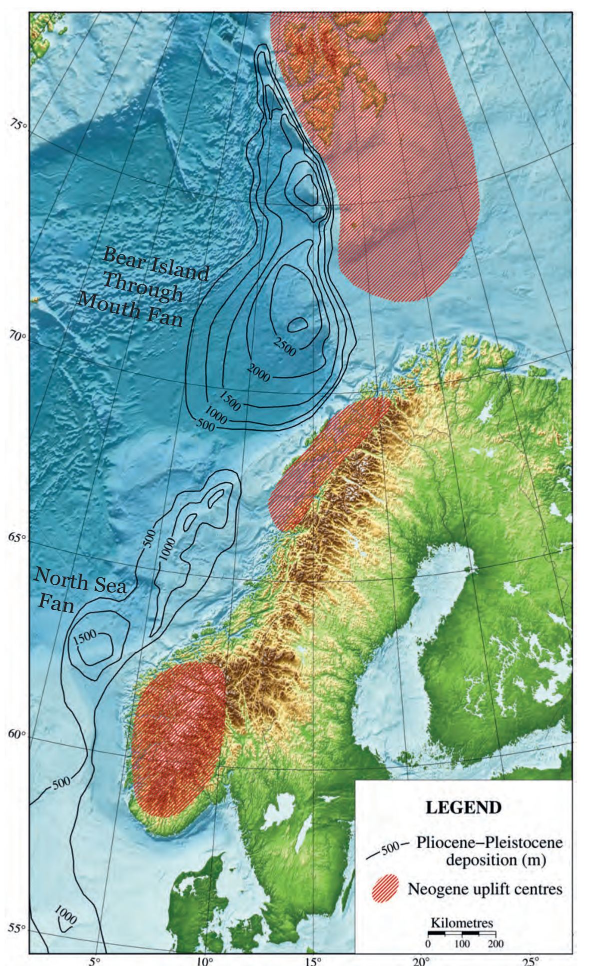

Figure 1: Neogene uplift centres and regions of Pliocene-Pleistocene deposition. The data are modified from Riis (1996), Faleide et al. (1996), Ottesen et al. (2010, 2014) and Henriksen et al. (2011).

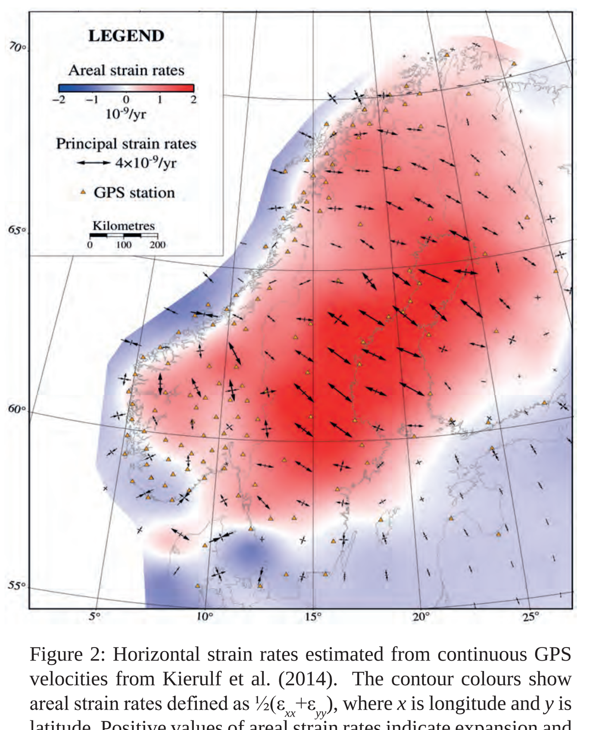

Figure 2: Horizontal strain rates estimated from continuous GPS velocities from Kierulf et al. (2014). The contour colours show areal strain rates defined as $\frac{1}{2}(\varepsilon_{xx}+\varepsilon_{yy})$, where x is longitude and y is latitude. Positive values of areal strain rates indicate expansion and negative values indicate contraction. The arrows show the principal strain rates, i.e. the largest and smallest strain rates in the horizontal plane. Figure modified from Keiding et al. (2015).

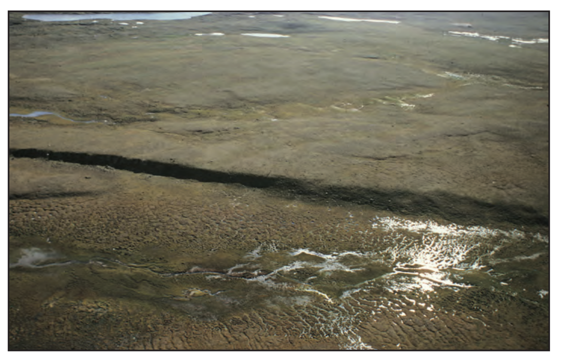

Figure 3: Aerial photo of the Stuoragurra fault in the Lapland Fault province, looking east, approximately 12 km NNE of Masi. The scarp has a maximum of 7 m height. Photo: Odleiv Olesen, 1989.

Reference to the map:
Keiding, M., O. Olesen, J. Dehls, 2018.
Neotectonic map of Norway and adjacent areas.
Geological Survey of Norway.

Projection: Transverse Mercator
Longitude of central meridian: 15° 0′ 00″
Latitude of central meridian: 0° 0′ 00″
Datum: WGS84

Acknowledgements: The map was produced as part of the NEONOR2 project. Dag Ottesen, Leif Rise, Fridtjof Riis, Henrik Mikko, Antti Ojala, Peter Japsen and Olav Vestøl contributed data or other information to the map.

References

Evans, D., Z. Harrison, P. M. Shannon, J. S. Laberg, T. Nielsen, S. Ayers, R. Holmes, R. J. Hoult, B. Lindberg, H. Haflidason, D. Long, A. Kuijpers, E. S. Andersen and P. Bryn, 2005. Palaeoslides and other mass failures of Pliocene to Pleistocene age along the Atlantic continental margin of NW Europe. Marine and Petroleum Geology 22, 1131–1148.

Faleide, J. I., A. Solheim, A. Fiedler, B. O. Hjelstuen, E. S. Andersen and K. Vanneste, 1996. Late Cenozoic evolution of the western Barents Sea-Svalbard continental margin. Global and Planetary Change 12, 53–74.

FENCAT, 2018. A joint Fennoscandian earthquake catalogue courtesy of University of Helsinki. Retrieved January 2018 from http://www.helsinki.fi/geo/seismo/english/bulletins/.

Heidbach, O., M. Rajabi, K. Reiter, M. Ziegler and WSM Team 2016. World Stress Map 2016. GFZ Data Services. http://doi.org/10.5880/WSM.2016.001.

Henriksen, E., H. M. Bjørnseth, T. K. Hals, T. Heide, T. Kiryukhina, O. S. Kløvjan, G. B. Larssen, A. E. Ryseth, K. Rønning, K. Sollid and A. Stoupakova, 2011. Uplift and erosion of the greater Barents Sea: impact on prospectivity and petroleum systems. Geological Society, London, Memoirs 35, 271–281.

Keiding, M., C. Kreemer, C. D. Lindholm, S. Gradmann, O. Olesen and H. P. Kierulf, 2015. A comparison of strain rates and seismicity for Fennoscandia: depth dependency of deformation from glacial isostatic adjustment. Geophysical Journal International 202, 1021–1028.

Kierulf, H. P., H. Steffen, M. J. R. Simpson, M. Lidberg, P. Wu and H. Wang, 2014. A GPS velocity field for Fennoscandia and a consistent comparison to glacial isostatic adjustment models. Journal of Geophysical Research 119, 1–17.

Laberg, J., S., and T. O. Vorren, 2000. The Trænadjupet Slide, offshore Norway - morphology, evacuation and triggering mechanisms. Marine Geology 171, 95–114.

Lagerbäck, R. and M. Sundh, 2008. Early Holocene faulting and paleoseismicity in northern Sweden. Geological Survey of Sweden, Research Paper C 836.

Mikko, H., C. A. Smith, B. Lund, M. V. S. Ask and R. Munier, 2015. LiDAR-derived inventory of post-glacial fault scarps in Sweden. GFF 137, 334–338.

Muir Wood, R., 1989. Extraordinary deglaciation reverse faulting in northern Fennoscandia. In: Gregersen, S., and P. W. Basham (eds.) Earthquakes at North-Atlantic Passive Margins: Neotectonics and Postglacial Rebound, NATO ASI Series, 141–173.

Olesen, O., H. Bungum, J. Dehls, C. Lindholm, C. Pascal and D. Roberts, 2013. Neotectonics, seismicity and contemporary stress field in Norway - mechanisms and implications. In: Olsen, L., O. Fredin and O. Olesen (eds.) Quaternary Geology of Norway, Geological Survey of Norway Special Publication 13, 145–174.

Olesen, O., M. Ask, D. Ask, J. F. Dehls, S. Gradmann, I. Janutyte, M. Keiding, H. P. Kierulf, T. R. Lauknes, C. Lindholm, Y. Maystrenko, J. Michalek, L. Olsen, L. Ottemöller, D. Ottesen, F. Riis, L. Rise, 2018. NEONOR2 final report – Neotectonics in Nordland – implications for petroleum exploration. NGU Report 2018.010.

Ottesen, D., L. Rise, E. S. Andersen, T. Bugge and T. Eidvin, 2010. Geological evolution of the Norwegian continental shelf between 61ºN and 68ºN during the last 3 million years. Norwegian Journal of Geology 89, 251–265.

Ottesen, D., J. A. Dowdeswell and T. Bugge, 2014. Morphology, sedimentary infill and depositional environments of the Early Quaternary North Sea Basin (56°–62°N). Marine and Petroleum Geology 56, 123–146.

Palmu, J.-P., A. E. K. Ojala, T. Ruskeeniemi, R. Sutinen and J. Mattila, 2015. LiDAR DEM detection and classification of postglacial faults and seismically-induced landforms in Finland: a paleoseismic database. GFF 137, 344–352.

Riis, 1996. Quantification of Cenozoic vertical movements of Scandinavia by correlation of morphological surfaces with offshore data. Global and Planetary Change 12, 331–357.

Solheim, A., K. Berg, C. F Forsberg and P. Bryn, 2005. The Storegga Slide complex: repetitive large scale sliding with similar cause and development. Marine and Petroleum Geology 22, 97–107.

Sutinen, R., E. Hyvönen, M. Middleton and T. Ruskeeniemi, 2014. Airborne LiDAR detection of postglacial faults and Pulju moraine in Palojärvi, Finnish Lapland. Global and Planetary Change 115, 24–32.

Talwani, M. and O. Eldholm, 1977. Evolution of the Norwegian-Greenland Sea. Geological Society of America Bulletin 88, 969–999.

Treimann, A. H., 2012. Eruption age of the Sverrefjellet volcano, Spitsbergen Island, Norway. Polar Research 31, 1–7.

Vestøl, O. et al., 2016. NKG2016LU – A new land uplift model for Fennoscandia and the Baltic region, courtesy of NKG Working Group of Geoide and Height Systems.